Effect of Surface Characteristics and Rainfall in Infiltration Rate: A Case Study of Kaligandaki River Basin

Janardan Joshi[1*]
[1]Assistant Professor, Faculty of Engineering, Far Western University, Nepal
[*]Corresponding Author: janardanjoshi16@fwu.edu.np; ORCID: https://orcid.org/0000-0003-4214-0231

Abstract

Study of infiltration characteristics is crucial for effective watershed management, as it helps determine the water availability for crops, the need of irrigation, groundwater recharge, and surface runoff. This study is aimed at identifying the relation between infiltration rate and surface characteristics as well as rainfall rate in the Kaligandaki River basin of Nepal using Hydrologic Modelling System (HEC-HMS). HEC-HMS is a physically based, semi-distributed model that uses the weather and spatial information of soil and landuse of the basin for deriving the inputs for the model. A hydrological rainfall-runoff model is developed for the Kaligandaki River basin, with outlet at hydrological station 420, Kotgau, of Department of Hydrology and Meteorology (DHM). The model was then validated at DHM station 420, Angsing, of Kaligandaki River. Model generated subbasin wise infiltration rates and existing landuse were analysed and it was found that subbasins with dominant landuse as forest had high infiltration rate among prevailing landuse types. Conversely, low infiltration rate was observed for barren area, snow/glacier and grassland landcover type dominated subbasins. A positive correlation among rainfall rate and infiltration rate was seen with linear increase in infiltration rate for an exponential increase of average rainfall intensity. Infiltration rate was found to have positive correlation with the Hydrologic Soil Group types as suggested by NRCS. Moreover, the study signified a greater impact of landcover over soil types on infiltration rates. Whereas, no significant impact of basin slope on infiltration rate could be identified, which may be due to preclusion of multiple topographic features. Understanding the impacts of rainfall intensity and surface characteristics on infiltration enables proactive measures to mitigate the issues like landslide and reduce flooding and soil erosion by improving infiltration rates through surface condition assessment.

Keywords: *Hydrological Modelling, HEC-HMS, Kaligandaki River Basin, Landuse and infiltration, Rainfall and infiltration*

Introduction

Rain falling on an unsaturated soil slope generates surface run-off after infiltration of some portion (Xue & Gavin, 2008). Water that runs off is mainly responsible for floods and other surface related events. Water required for vegetation growth and ground water supply replenishing to streams, springs and wells is fulfilled by the infiltrated water Rawls et. al. (1993). Turner (2006) has defined infiltration as the perforation of water, with snow, rainfall and irrigation as its source, into the soil from its surface and below. Surface run-off quantification and determination of underground movement and storage of water within a watershed can be studied by understanding infiltration process and the factors affecting it (Skaggs & Khaleel, 1982). Infiltration plays a vital role in soil-water interaction. The ability to quantify infiltration also plays a vital role in determining the availability of water for growth of crop and to estimate the amount of supplementary water required for irrigation purpose. Upon understanding the effects of rainfall intensity on infiltration, measures can be taken to warn the possible consequences like landslides. Proper assessment of interaction of surface conditions and infiltration can help reduce flooding and soil erosion caused by surface run-off by increasing the infiltration rates.

Vegetation and natural surface covers play a vital role in increasing infiltration capacity of the soil. Peat and mulches like surface covers reduce evaporation from the surface of soil and they also help maintain temperature whereas, vegetation covers aid the loss of moisture through evapotranspiration. Vegetation loosens the soil with growth of roots. Peat and mulches like surface covers and vegetation also prevent the damage of surface soil structure (crusting and surface sealing) by intercepting the direct impact of drops of rain.

Infiltration rate is also affected by surface slope. With an increase in surface slopes, covered with grass, a reduction if infiltration rate was seen (Haggard, Moore Jr., & Brye, 2005). According to Haggard, Moore Jr., & Brye (2005), for soil moisture near to saturation, soil slopes may have the largest impact on rate of water infiltration and surface run-off generation. Also higher rates of infiltration have been observed in sloping lands without cover in comparison to flat lands without cover (Poesen, 1984). This outcome can be due to lowered surface sealing of land, as higher open pores are formed in larger amount of suspended sediments due to high surface flow velocities (Romkens et. al., 1995).

Instantaneous rate of rainfall is termed as rainfall intensity. The ratio of total rainfall depth and its duration gives rainfall intensity for a uniform storm. In cases without surface ponding, the maximum infiltration rate called "the infiltration capacity" by Horton (1940) or "infiltrability" by Hillel (1971), "equals or exceeds the rainfall intensity and thus, the rainfall intensity provides the upper limit for the infiltration rate". For a given intensity of rainfall, R, the soil profile reaches a constant water content θL, where θL is the water content with the hydraulic conductivity, K, equal to the rainfall rate, R, i.e. K (θL) = R. "Since unsaturated hydraulic conductivity increases with increasing water content, the higher the rainfall intensity, the higher the value of θL" (Skaggs & Khaleel, 1982).

Varying infiltration rates for groundwater recharge were studied by Joshi & Shrestha (2008) in Patan area of central Nepal. In this study they found out that the infiltration rates increased remarkably during the dry periods of winter and the pre-monsoon periods whereas decreased during the early winter and summer periods. The impact of land use/cover change in groundwater recharge in Kathmandu Valley, Nepal have been studied (Lamichhane & Shakya, 2019). This study used in-situ field tests as well as analysis of infiltration rates for identifying the impact. Surface runoff and impact of rain drops can be slowed down by vegetation growth and thus infiltration rates can be maintained (Chalise, Kumar, & Kristiansen, 2019). This study has also suggested that mulching facilitates water infiltration in to the soil by reducing surface runoff.

Methods for modelling infiltration are generally categorized in three classes as approximate models, empirical models and physically based models. Solution of the Richard's equation is required in the physically based processes (Richards, 1931). Richard's equation has described the flow of water in soils in respect to their hydraulic conductivity. It has also described water pressure in the soil in terms of water content of soil for defined boundary conditions. The solution of Richard's equation for various flow problems that need numerical methods and input data in detail is highly challenging (Rawls et. al., 1993). On the other hand empirical models seem to be controlled more by their calibration conditions but constrained less by soil surface and profile assumptions, the reason being the estimation of infiltration parameters by actual field-observed infiltration data (Hillel, 1988), (Skaggs & Khaleel, 1982). All the infiltration equations make use of At least some parameters are used in defining infiltration in every infiltration equations. But the higher physically-based equations tend to depend more on the physical and hydraulic properties existing in the soil profile, like gradient of soil moisture, wetting front suction and hydraulic conductivity in saturated condition.

Landuse/cover type, soil type, basin characteristics and rainfall intensity can be used directly/indirectly as input parameters for Hydrologic Engineering Centre – Hydrologic Modelling System (HEC-HMS) model (Scharffenberg et. al, 2010). Rainfall data can be acquired from available observed datasets. Basin characteristics can be identified with the help of Digital Elevation Model (DEM) data of the region. Landuse/cover and soil data can be acquired from various freely available online sources. Infiltration rates need to be simulated, from HEC-HMS model, to study its response to rainfall rates, landuse/cover, soil types and basin slope. This study is aimed at identifying the relation and response of infiltration rates to surface characteristics and rainfall rates the Kaligandaki River basin of Nepal. Relationships between landuse types, soil types, rainfall intensity, and basin slope and infiltration rates have been studied in detail.

Objectives

The broader objective of this study is to study the relation of infiltration rate with surface characteristics and rainfall rate of the Kaligandaki River basin.

Specific objectives of this study have been listed below.

- To study the response and relation of infiltration rates to surface characteristics of the basin i.e. landuse/cover type, soil type and basin slope
- To study the relation of varying rainfall rates with infiltration rates.

Materials and Methods

Study Area

The study area is the Kaligandaki River basin, extending from the Himalayan range in the north to northern borders of Palpa and Nawalparasi districts in the south. The Kaligandaki Basin covers 11 districts of the country. Location of the Kaligandaki River basin is presented in Figure 1. Major tributaries of the Kaligandaki baisn include Kaligandaki, Modi Khola, Myagdi Khola and Andhi Khola rivers. This basin extends from Latitude 270 43’ to Latitude 290 20’ and Longitude 820 53’ to longitude 840 22’ covering an area of 11,744 sq. km. The average annual rainfall in the basin is 2047mm. The Kali Gandaki River drains the area from the higher Himalayas to central Nepal cutting the higher Himalayan range through the deepest gorge in the world, 5,000m deep, between Annapurna and Dhaulagiri (Parajuli, 2016). The temperature records fall as low as -6.30C in Jomsom in the northernmost part of the basin.

The basin has a diverse climate, ranging from arid tundra at highest altitudes, through alpine, cold temperate, warm temperate and subtropical with decreasing altitude, with a monsoon climate in the lowest areas (Manandhar, Pandey, & Kazama, 2012). The basin has forest type as dominant land cover area followed by agricultural area.

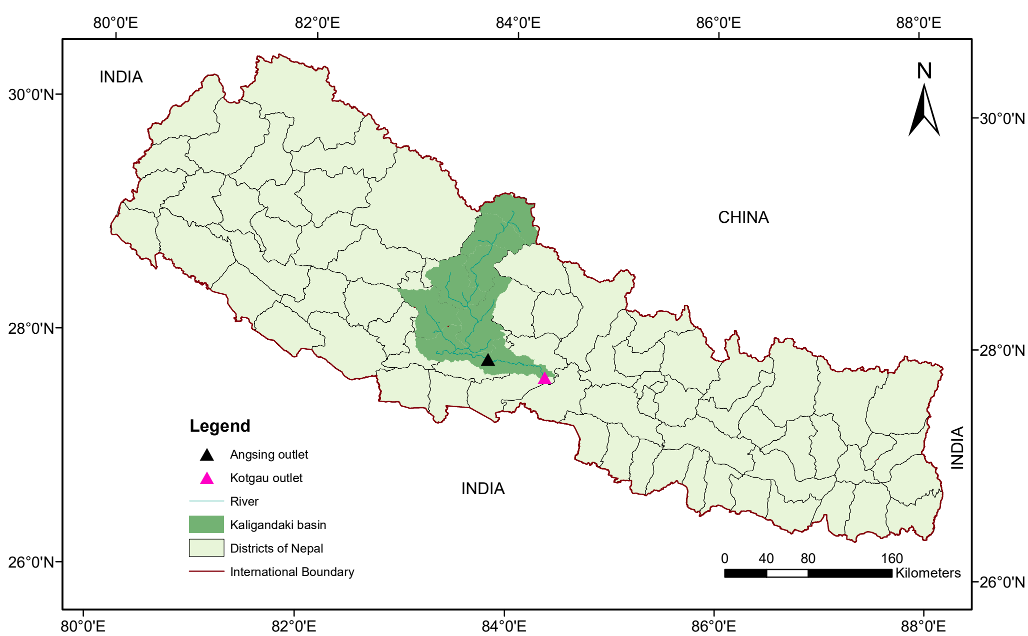

Figure 1 Location Map of study area

Details of the hydrological gauge stations considered in the study, Kotgau and Angsing, are shown in Table 1.

Table 1 Features of gauge points studied

S. No.	Gauge Point	Latitude (degrees)	Longitude (degrees)	Elevation (m)	Basin Area (sqkm)	Avg. annual rainfall(mm)
1.	Angsing	27.89	83.8	351.05	10,796	2031
2.	Kotgau	27.75	84.345	198	11,744	2047

Data Acquisition

HC-HMS requires subbasin wise aggregated input data for model set-up and watershed simulations. HEC-HMS being a semi-distributed model, only subbasin wise data is required. To extract the subbasin wise data we need various spatial datasets in a recognizable format by the model. This makes data collection and preparation a time consuming and challenging step of the study. Given below is the list of spatially distributed data required in the HEC-HMS model as direct or indirect input;

Digital Elevation Model (DEM)

A 90m resolution raster DEM developed by USGS (United States Geological Survey), was used for the purpose of this study. The same DEM clipped to represent the watershed is shown in Figure 2.

Landuse/cover data

The landuse map required for the study area was extracted from Landuse map of Nepal published by ICIMOD (2010) in digital format. Landuse map is used to produce Curve Number (CN) grid which is a parameter for determining basin lag time and surface runoff. Figure 3 represents the various landuse types existing in the study basin. Landuse type throughout the basin is dominated by Forest (31.23%), followed by Agriculture (26.87%), Barren area (15.4%), Snow/glacier (13.46%), Grassland (10.43%), Shrubland (2.29%), Water body (0.27%) and Built-up area (0.04%).

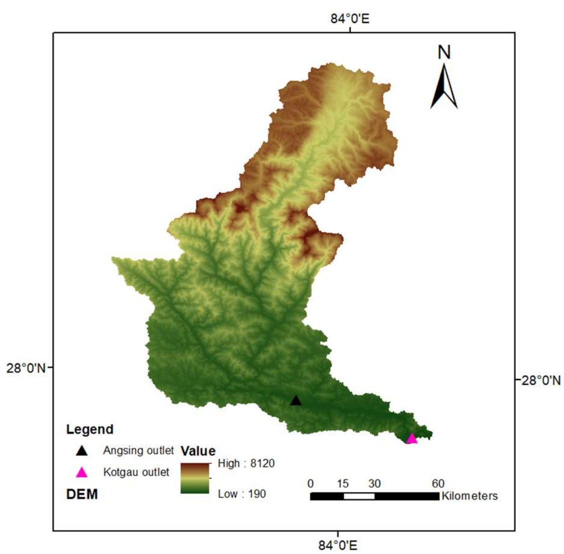

Figure 2 Digital Elevation Model (DEM)

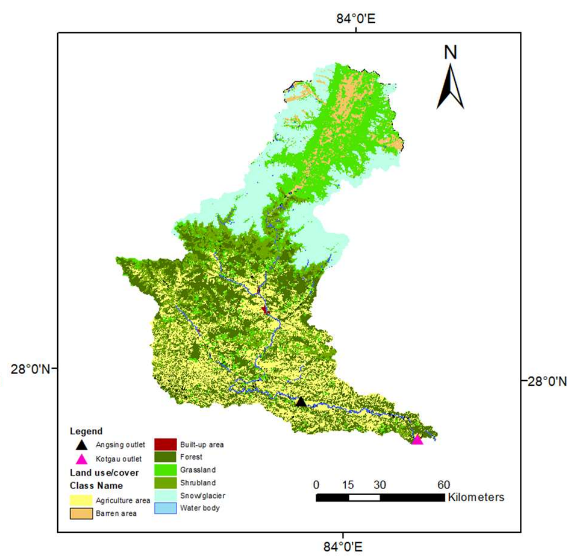

Figure 3 Landuse/ cover map of the study basin

Soil Type

The soil type data was acquired from the FAO soil properties database and Soil and Terrain (SOTER) database for Nepal. This model required Hydrologic Soil Group (HSG) classification as per Natural Resources Conservation Service (NRCS) and thus it was extracted from available soil maps and database. Figure 4 represents the HSG classification as per NRCS. Hydrological Soil Group B (Silt loam or loam) (71.5%) is prominent followed by A (sandy loam or loamy sand) (28.21%) and C (sandy clay loam, clay loam, silty clay loam or sandy clay) (0.29%).

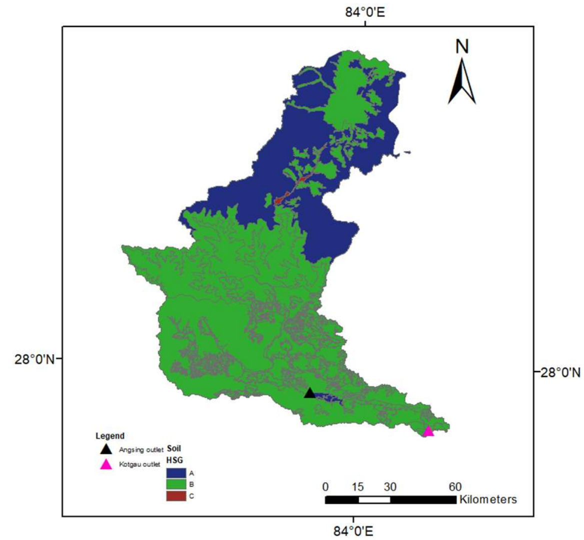

Figure 4 HSG types in the study basin as per NRCS classification

Meteorological Data

Climate data to be used in the model are daily precipitation (mm), daily mean temperature (^{0}C), relative-humidity (RH) (%), wind velocity (m/s) and maximum daily sunshine hours. Among these climate data daily precipitation data was used as precipitation input in the HEC-HMS model and rest of the climate data, daily mean temperature, relative-humidity, wind velocity, and maximum sunshine hours, were used for calculating potential evapotranspiration by Penman's method (Penman, 1948). These data were acquired from Department of Hydrology and Meteorology (DHM). Due to scarce DHM meteorological .stations in the northernmost region of the basin, Climate Forecast System Reanalysis (CFSR) Global Weather data was used. The spatial scattering of the meteorological stations used in the study basin are represented in Figure 5. In order to represent the spatial variability of the climatic data, daily spatially weighted average values for each sub-basin is calculated from the available point information of selected meteorological stations using Thiessen's Polygons.

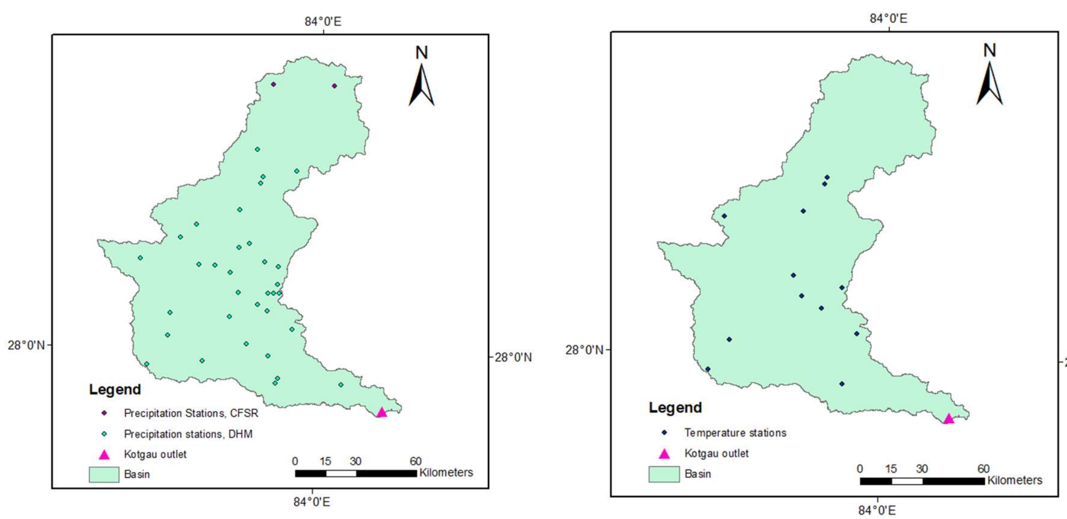

(a) Precipitation stations in the basin

(b) Temperature stations in the basin

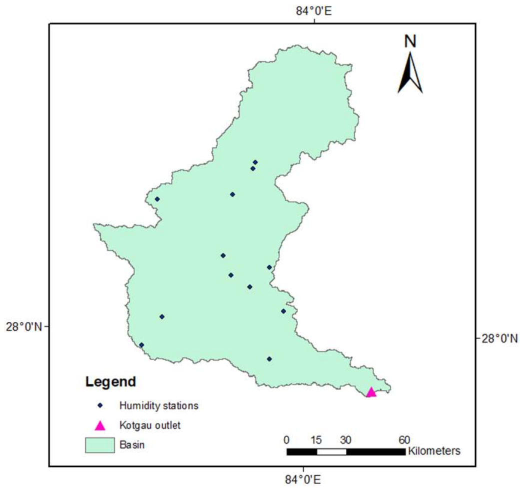

(c)Humidity stations in the basin

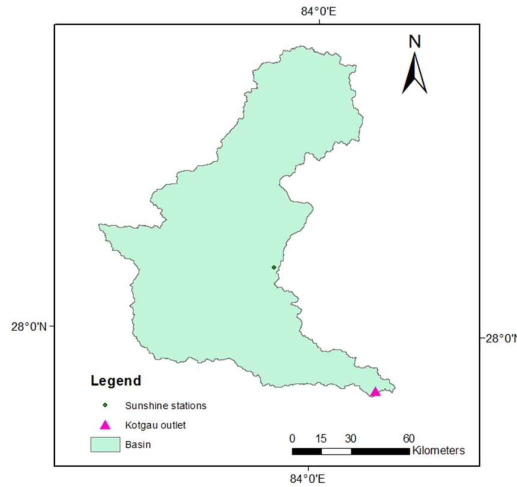

(d) Sunshine stations in the basin

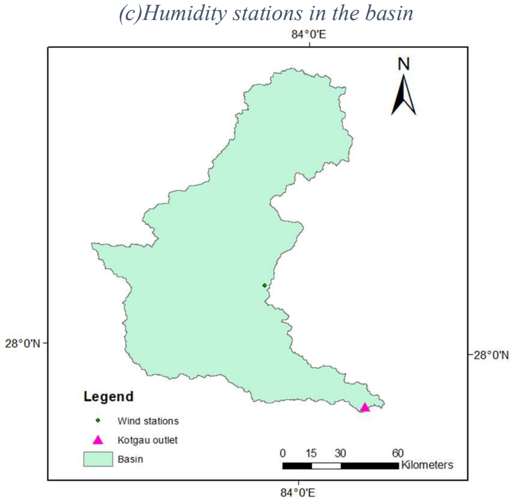

(e) Wind stations in the basin

Figure 5 Meteorological data stations in the basin

Hydrological Data

The hydrological data were collected from the hydrology section of the DHM. Table 2 shows the details of the Hydrological outlet station of Kaligandaki basin.

Table 2 Location details hydrological stations considered in the study

S. No.	Station No.	Gauge Point	Latitude (degrees)	Longitude (degrees)	Elevation (m)	Data Year
1.	419	Angsing	27.89	83.8	351.05	1998-2003, 2008-2011
2.	420	Kotgau	27.75	84.345	198	1998-2003, 2008-2011

Model Setup

The Hydrologic Modelling System (HEC-HMS) develops meteorological model and basin model for simulating hydrologic process. Basin characteristics comprise of hydrograph transformation, losses in soil, base-flow component and routing of river reach. These characteristics are input by the user which represents a basin model. Meteorological model guides the process of evapotranspiration occurring in the watershed. It also dictates the application of precipitation, which may be snow or rainfall, in basin model. The rainfall runoff process in the study basin is then defined by the meteorological and basin models in tandem (Scharffenberg et. al., 2010).

Data Extraction for developing HEC-HMS model

HMS project setup and basin processing

Terrain preprocessing is done in Arc-GIS to generate river network and sub-basins for hydrological model in HEC-HMS. The HMS project area is generated by the selection of the main outlet of the Basin as a project point in the flow accumulation map. The stream gauging station at Kotgau is considered as the control point for the project generation. The study area has been sub-divided into 8 subbasins.

SCS Curve Number grid development

SCS curve number for a watershed is developed using landuse/cover and soil data. SCS CN grid development involves preparing landuse data and soil data, merging landuse and soil data, creating CN look-up table and finally development of CN grid.

HMS model generation

The entire catchment is depicted into HEC-HMS in the form of Basin Model. The HMS basin model to be used in HEC-HMS is generated including background map of basin and river network as represented in Figure 6.

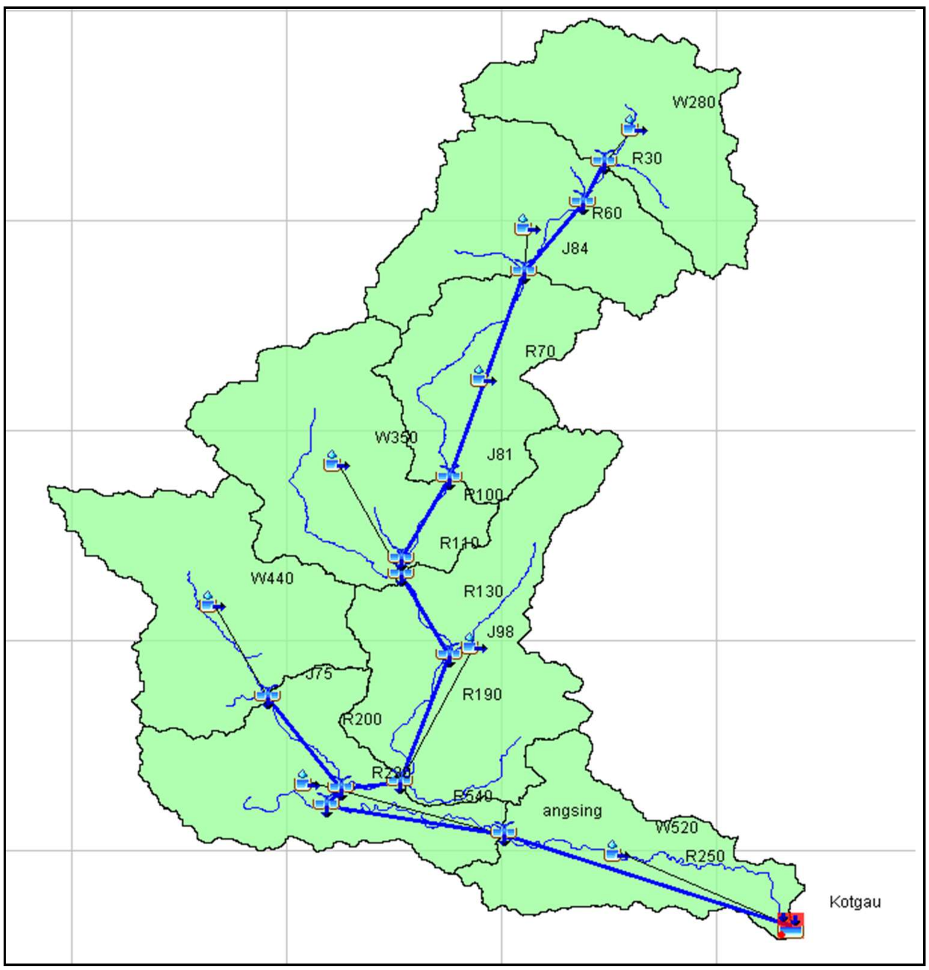

Figure 6 Generated HMS model

Calculating Potential Evapotranspiration (PET)

Penman's method has been used for determining monthly potential evapotranspiration (PET) required for the model. Penman's method, integrating some changes proposed by other scientists is (Subramanya, 2008),

$$PET = \frac{AH_n + E_a\gamma}{A + \gamma}$$

PET = daily potential evapotranspiration in mm/day
A = slope of the saturation vapour pressure vs temperature curve at the mean air temperature, in mm of mercury per 0C
Hn = net radiation in mm of evaporable water per day
Ea = parameter including wind velocity and saturation deficit
γ = psychrometric constant = 0.49 mm of mercury/0C

Calculating sub-basin lag time

Time deferral between the precipitation events on a basin to the peak runoff is calculated as subbasin lag time. Simas (1996) has approximated lag time for typical natural catchment and nearly even run-off distribution as;

$$L_t = 0.6T_c$$

Where, Lt = lag time in hours

Modelling of watershed in HEC-HMS

Basin Model

The basin model is imported in HMS as hydrologic network that contains HMS model elements and their connectivity. For rainfall-runoff simulation, models for each hydrologic process is selected in the HMS model setup. Following methods are selected to aid the rainfall-runoff simulation:

Canopy: Simple canopy

Surface: Simple surface

Base flow model: Constant monthly baseflow

Loss model: Green & Ampt loss model

Runoff transform model: SCS unit hydrograph method

Channel routing model: Muskingum model

Meteorological model

This model serves the principle purpose preparing meteorological boundary conditions in sub-basins. The gage weight model is used to represent rainfall in the basin. The parameters that describe the gages to be used and the gage weight to be applied are specified individually for every sub-basin. The gage weights for selected eight gauge stations are used in this study. Also monthly PET values estimated by Penman's method have been used in the meteorological model to represent the PET.

Results and Discussion

Model summary

The model was initially calibrated and validated at Kotgau (DHM st. no. 420). The model was also found valid at Angsing (DHM st. no. 419.1) in Kaligandaki River, owing to the rationality of parameters throughout the basin. During the calibration process a good fit was observed with NSE, R^2 and PBIAS values of 80.03%, 0.81 and 11.76% whereas the simulated volume was underestimated by 11.8%. The volume underestimate is within the limits suggested by (Najim, Babel, & Loof, 2006), who recommended that the percent variation in simulated and observed values within 20% is acceptable. During the validation at Kotgau a good fit was observed with NSE, R^2 and PBIAS values of 81.66%, 0.80 and 3.21% whereas the simulated volume was underestimated by 3.2%. Similarly, the model was validated at Angsing with NSE, R^2 and PBIAS values of 67.54%, 0.68 and -0.23% whereas the simulated volume was overestimated by 0.2% which is within the limits.

Flow calibration at Kotgau

Calibration of the simulated discharge with the daily observed data, at Kotgau gauging station, was performed for a time-period of six years starting from January 1998 to December 2003. The summary of calibration results along with Nash-Sutcliffe Efficiency (NSE) is presented in Table 3 below.

Table 3 Statistical parameters for flow calibration at Kotgau

Outlet	Cumulative volume (10^6m³)		Average Flow (m³/s)		Model efficiency			Run Period
	Observed	Simulated	Observed	Simulated	NSE	R^2	PBIAS	
Kotgau	96398.92	85062.35	509.23	449.35	80.03%	0.81	11.76%	1998-2003

Figure 7 and Figure 8 represent the hydrograph and scatterplot for flow calibration at Kotgau.

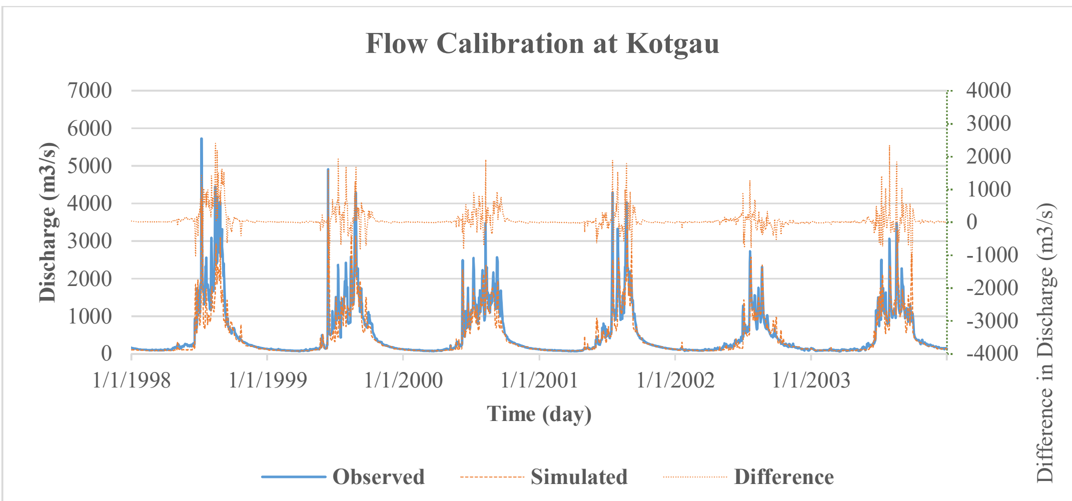

Figure 7 Flow calibration hydrograph at Kotgau

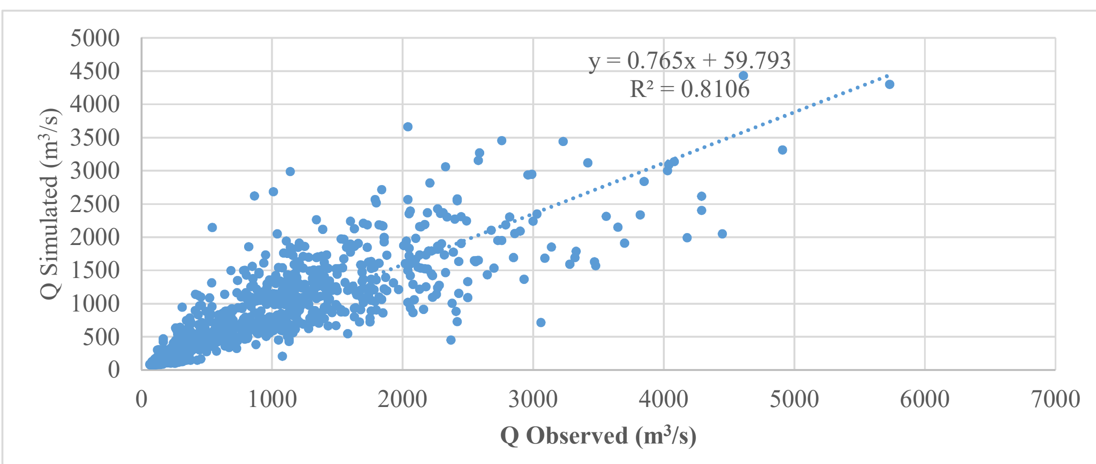

Figure 8 Scatterplot for flow calibration at Kotgau

Table 4 Statistical parameters for flow validation at Kotgau

Outlet	Cumulative volume ($10^6 m^3$)		Average Flow (m^3/s)		Model efficiency			Run Period
Kotgau	Observed	Simulated	Observed	Simulated	NSE	R^2	PBIAS	2008-2011
	56776.24	54951.97	449.78	435.33	81.66%	0.80	3.21%	

Figure 9 and Figure 10 below are the scatterplot and hydrographs respectively.

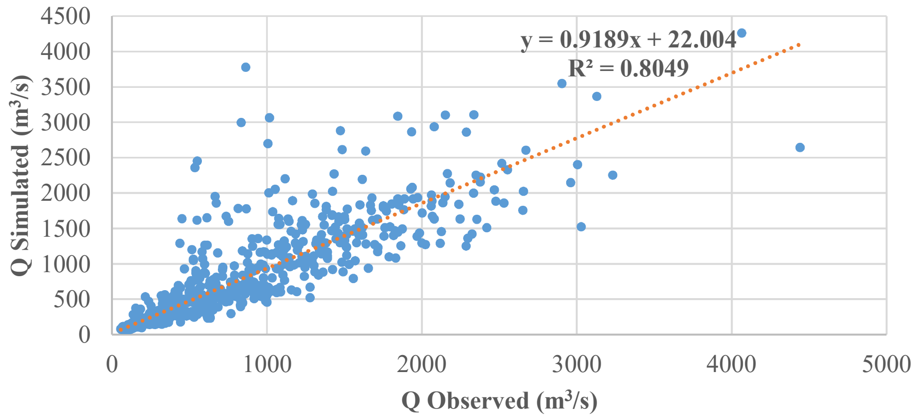

Figure 9 Scatterplot for flow at validation at Kotgau

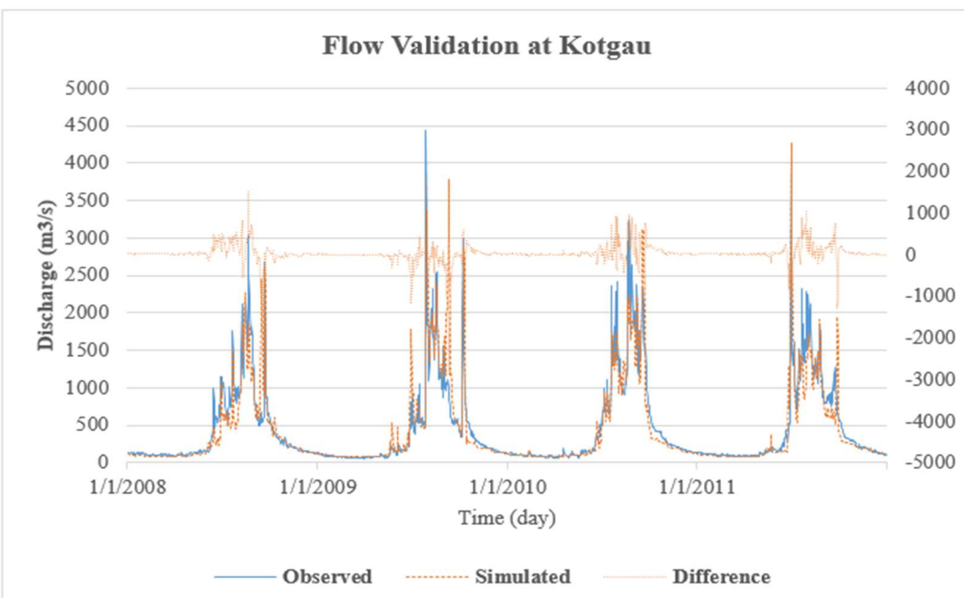

Figure 10 Flow validation hydrograph at Kotgau

Flow validation at Angsing

The fitted parameters for rainfall runoff modelling in Kotgau basin were then further validated for the Kaligandaki basin at Angsing, a gauging station upstream of Kotgau in Kaligandaki. The summary of validation results along with NSE is presented in Table 5 below. Figure 11 and Figure 12 below are the scatterplot and hydrographs respectively.

Table 5 Statistical parameters for flow validation at Angsing

Outlet	Cumulative volume ($10^6 m^3$)		Average Flow (m^3/s)		Model efficiency			Run Period
Angsing	Observed	Simulated	Observed	Simulated	NSE	R^2	PBIAS	2008-2011
	49600.84	49713.75	392.94	393.83	67.54%	0.68	-0.23%	

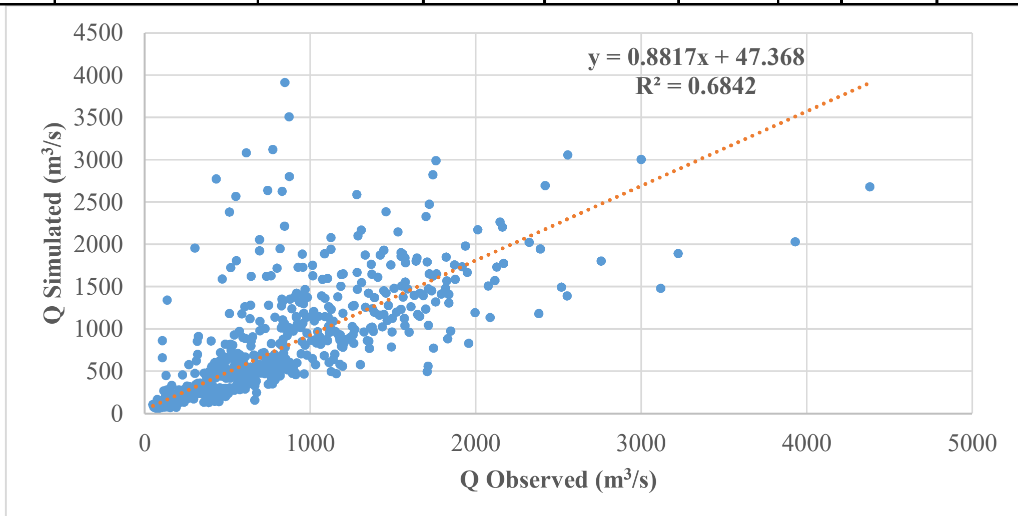

Figure 11 Scatterplot for flow validation at Angsing

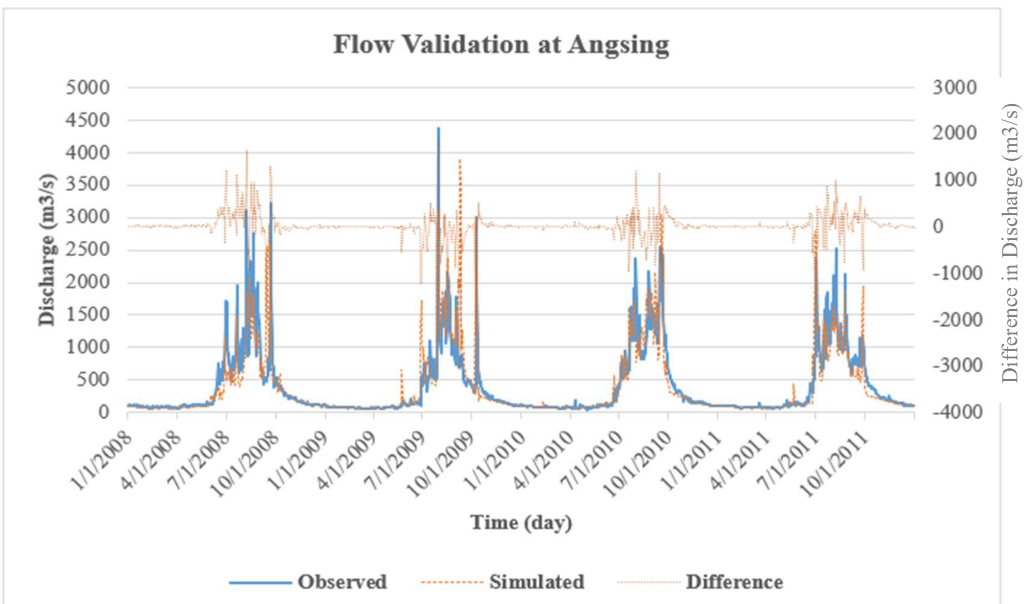

Figure 12 Flow validation hydrograph at Angsing

The precipitation data available was daily only. And thus the model was calibrated and validated for daily data. From the developed daily model, daily infiltration values were extracted. These values can be extracted using HEC-DSSvue from the simulation result files in the parent folder. From the extracted daily infiltration data, hourly infiltration rates were computed by dividing the total daily infiltrated water by duration of day in hours. Similarly, rainfall intensity in mm/hr was calculated by dividing the daily rainfall data by duration of the day in hours. "If the rate of rainfall is less than the saturated hydraulic conductivity for the soil, infiltration may continue indefinitely at the rainfall rate without the occurrence of ponding" (Turner, 2006). Turner (2006) concluded that saturated hydraulic conductivity, used in Green & Ampt method, has high sensitivity in modelling infiltration. After the calibration and validation of the model, simulated infiltration values were extracted and analyzed for relations with landuse, soil types, basin slope and rainfall. Results, thus obtained have been discussed in the upcoming sections.

Infiltration rate and Landuse

Subbasin wise landuse data was identified and infiltration rates were also calculated for each subbasins. Forest (31.23%) was the dominant landuse throughout the study area. Subbasins 4, 5 and 6 had forest area (>50%) as major landuse. Infiltration rates for these subbasins were found to be higher (as high as 43% above mean value) as shown in Figure 13 Landuse vs. average infiltration rate in the basin. The results are seen to be consistent with findings from previous studies, which have shown that areas with dominant forest cover have higher infiltration rates (Ibeje & Osuwagwu, 2000), (Yimer et. al., 2008), (Landon, 1991), (Cardwell, 2017), (Poulenard et. al., 2001). Infiltration rates for subbasin 7 and subbasin 8 were around only 6% higher than average infiltration rates. These subbasins had significant agriculture area. Changes in soil bulk density, organic content (Yimer et. al., 2008) and changes in structural stability of the soil (Celik, 2004) can be the possible reasons of higher infiltration rates in Forest covered areas as compared to Agricultural areas. Subbasins with snow/glacier, barren area and grassland as prominent landuse types were seen to have lower infiltration rates (about 38% below average values). The summary of variation in average infiltration rates of each subbasin from the basin average is presented in Table 6.

Table 6 Deviation of average subbasin infiltration rates from average of basin

Subbasin	Deviation of avg. Infiltration rate from basin avergae
SB1	-21.4%
SB2	-38.7%
SB3	-37.2%
SB4	6.1%
SB5	43.0%
SB6	14.7%
SB7	10.8%
SB8	2.1%

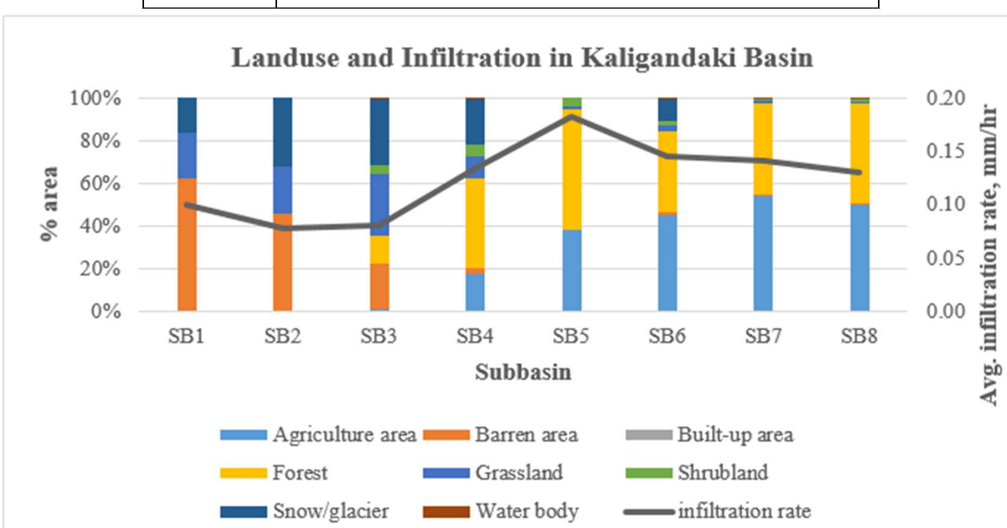

Figure 13 Landuse vs. average infiltration rate in the basin

Infiltration and Soil Type

Hydrologic Soil Groups for each subbasins were identified. HSG type B (silt loam or loam) was found dominant in the southern region of the basin and HSG type A (sandy loam or loamy sand) was prevalent in the northern region of the basin with traces of HSG type C (sandy clay loam, clay loam, silty clay loam or sandy clay). NRCS has categorized these soil groups according to infiltration rates also. Subbasin wise infiltration rates were not found to have significant relation with the soil types as defined by the NRCS. We have used Green & Ampt method to simulate the infiltration process and saturated hydraulic conductivity of the soil used in this method is highly sensitive (Turner, 2006). Spatial heterogeneity of saturated hydraulic conductivity of the soil (Russo & Bresler, 1982), unlike in Green & Ampt loss model, can be the reason for weak correlation of infiltration rates with Hydrologic Soil Group. The infiltration rates versus soil group types is shown in Figure 14. This effect can also be explained as dominance of landuse/cover over the soil group type regarding infiltration rates. Yimer et. al. (2008) assumed soil texture and bulk density to have less effect in infiltration rates due to low variation in soil properties in the study area which is also observed in our model.

Infiltration rate and Basin slope

Average basin slope was determined for each subbasin and relation and dependency of infiltration rates with subbasin slopes was studied. Specific relation of basin slope with infiltration rates could not be identified except for sub-basin 3 which had lowest infiltration rates with highest basin slope. Steeper slopes tend to have lower infiltration rates due to reduced contact period with the soil surface (Ansari, Katpatal, & Vasudeo, 2016). The average basin slope versus average infiltration rate plots have been shown in Figure 15. The differences in average basin slopes found in the present study are fairly small. Studies (Godsey & Elsenbeer, 2002; Zimmermann & Elsenbeer, 2008) showed variation of infiltration capacities on various slope aspects. Yimer et. al. (2008) suggested to consider multiple topographic features for studying the impact of slope position on infiltration.

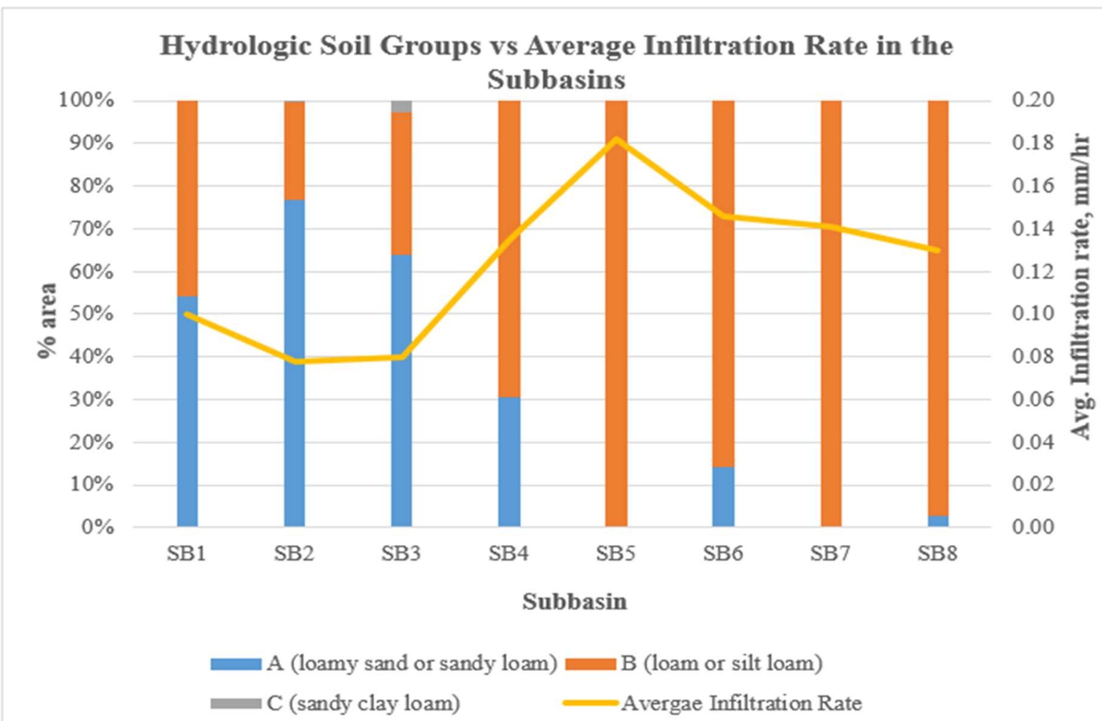

Figure 14 Hydrologic Soil Group vs. average infiltration rates in the subbasins

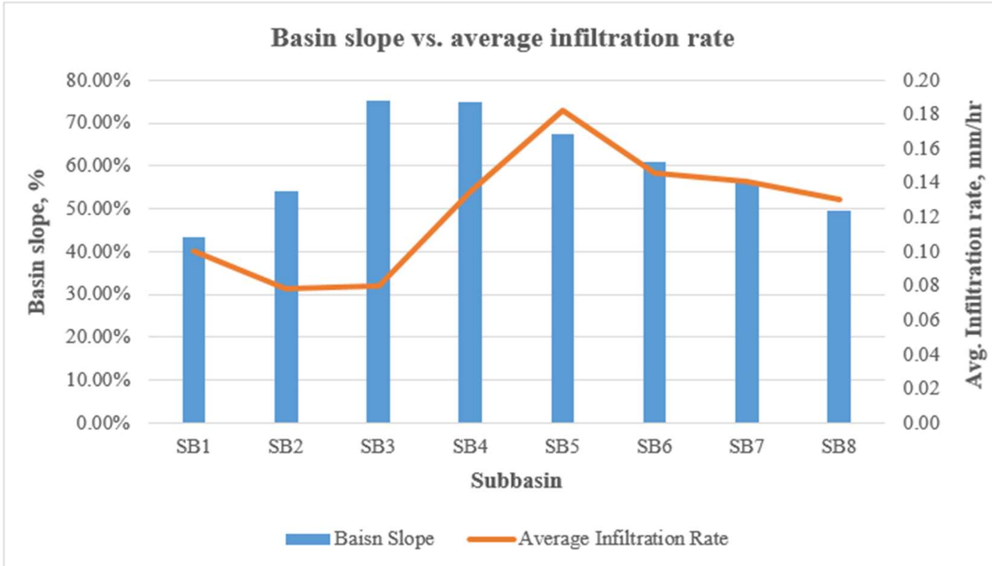

Figure 15 Basin slope vs. average infiltration rate

Infiltration rate and Rainfall intensity

Average rainfall intensity was calculated for each subbasin for every intervals of standard deviation and corresponding infiltration rates were also averaged. This average rainfall rate vs average infiltration rate showed an exponential trend line with R^2 values greater than 0.8 for all the subbasins. This exponential trendline suggested that for exponential increase in rainfall rate there was linear increase in infiltration rate. And this exponential increase was pronounced for extreme rainfall rates as seen in subbasins 1, 2, 5 and 6. This linear increase in infiltration rates for exponential increase in rainfall intensity can be due to the surface sealing and surface compaction for high rainfall intensities. Precipitation of longer duration, more frequent and lower intensity tends to have higher recharge potential (LaMoreaux et. al., 2009). A sample for infiltration rate versus rainfall intensity for standard deviation intervals plot has been shown in Figure 16. Input precipitation data was daily and thus infiltration rate decay curve ((Govindraju, Morbidelli, & Corradini, 2001), (Corradini, Govindaraju, & Morbidelli, 2002), (Gavin & Xue, 2008)) could not be studied. The study of infiltration rate decay curve could have provided a clearer insight to the infiltration process as infiltration is a continuous process, unlike our assumption of lumped daily infiltration.

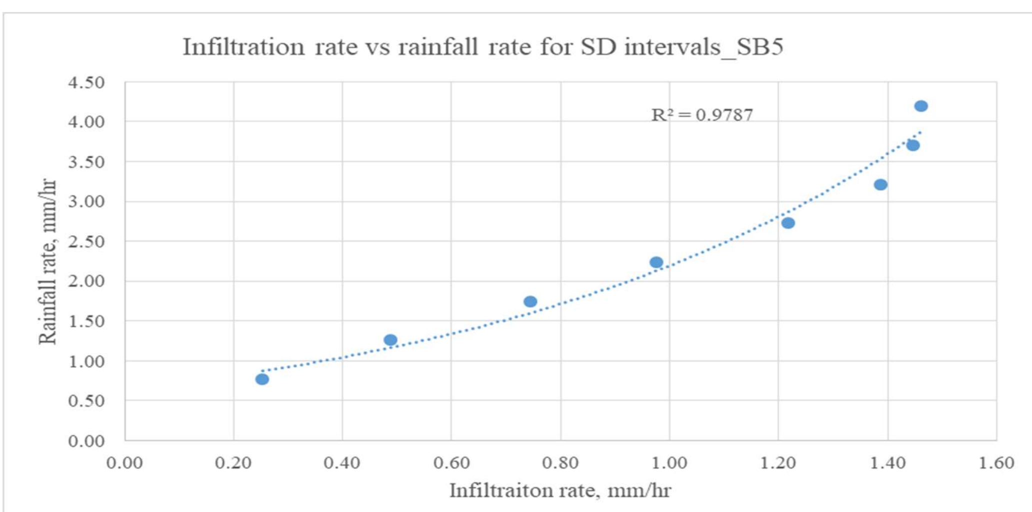

Figure 16 Infiltration rate vs. rainfall intensity plot

Conclusion

The current study aims to present the interaction of infiltration with surface characteristics via integrated use of numerical modelling tools and spatial data for large watershed. A rainfall-runoff model was developed in Kaligandaki River basin using HEC-HMS. Basin landuse/cover, soil, slope and rainfall data were then studied in conjunction with infiltration rates estimated from the model. The model was validated with satisfactory statistics suggesting that Green & Ampt, as loss method, and SCS CN method, as transform method, can be used with satisfactory results in the Kaligandaki River basin.

The study found that subbasins with landcover dominated by forests had notably higher infiltration rates, while those with barren areas, snow/glaciers, and grasslands had lower rates. Agricultural areas exhibited a lower infiltration compared to forests, possibly due to differences in soil structural stability. The subbasin-wise infiltration rates did not strongly correlate with the identified Hydrologic Soil Group (HSG) types as defined by the NRCS. The weak correlation between infiltration rates and HSG types may be attributed to spatial variations in soil conductivity and the dominance of land use/cover in influencing infiltration rates, consistent with previous research findings. Rainfall intensity was found to have an exponential relationship with infiltration rate. Basin slope was not found to have any dominating effect in contrast to the effects of landuse and soil type in infiltration. The small variation in basin slope among various subbasins can be the reason. Literatures drawing similar conclusion have suggested to consider multiple topographic features for studying the impact of slope position in infiltration. Experimental setups for the study of infiltration rate decay curve can significantly validate few of the findings of this study.

Conflict of interest

Author declares no conflict of interest.

References

Ansari, T. A., Katpatal, Y. B., & Vasudeo, A. D. (2016). Spatial evaluation of impacts of increase in impervious surface area on SCS-CN and runoff in Nagpur urban watersheds, India. *Arab J. Geosci, Vol. 9*. doi:DOI 10.1007/s12517-016-2702-5

Cardwell. (2017). *The effect of landuse on infiltraiton in Taita Hills, Kenya.* Helsinki: University of Helsinki, Department of Geosciences and geography.

Celik, I. (2004). Land-use effects on organic matter and physical properties of soil in a southern Mediterranean highland of Turkey. *Soil and Tillage Research*, 8.

Chalise, D., Kumar, L., & Kristiansen, P. (2019). Land Degradation by Soil Erosion in Nepal: A review. *soil systems*, 18.

Corradini, C., Govindaraju, R., & Morbidelli, R. (2002). Simplified modelling of areal average infiltration at the hillslope scale. *Hydrological Processes*.

Gavin, K., & Xue, J. (2008). A simple method to analyse infiltration into soil slopes. *Comput Geotech*, 8.

Godsey, S., & Elsenbeer, H. (2002). The hydrologic response to forest growth: a case study from southwestern Amazonia. *Hydrological Processes*.

Govindraju, R., Morbidelli, R., & Corradini, C. (2001). Areal infiltraiton modelling over soils with spatially correlated hydraulic conductivities. *Journal of Hydrologic Engineering, ASCE. Vol. 6*, 9.

Green, W., & Ampt, G. (1911). Studies of soil physics, Part 1. The flow of air and water through soils. *Journal of Agricultural Science*, 24.

Gupta, H. V., H., K., Yilmaz, K., & Martinez, G. F. (2009). Decomposition of the mean squared error and NSE performance criteria: Implications for improving hydrological modelling. *Journal of Hydrology*, 12.

Haggard, B., Moore Jr., P. A., & Brye, K. R. (2005). Effect of slope on runoff from a small variable slope box. *Journal of Environment Hydrology*, 9.

Hillel, D. (1971). *Soil and water: Physical principles and processes.* New York: Academia Press.

Hillel, D. (1988). *Environmental soil physics.* San Diego: Academic Press.

Horton, R. (1940). An approach towards a physical interpretation of infiltraiton capacity. *Soil Science Society of America*, 19.

Ibeje, A., & Osuwagwu, J. O. (2000). Impacts of landuse of infiltration. *World Journal of Engineering Research and Technology*, 8.

Joshi, H. R., & Shrestha, S. D. (2008). Feasibility of Recharging Acquifer through Rainwater in Patan, Central Nepal. *Bulleitin of the Department of Geology, 11*, 41-50.

Knoben, W., Freer, J., & Woods, R. (2019). Technical note: Inherent benchmark or not? Comparing Nash-Sutcliffe and Kling-Gupta efficciency scores . *Hydrology and Earth System Sciences*, 9.

Lamichhane, S., & Shakya, N. M. (2019). Alteration of groundwater recharge areas due to land use/cover change in Kathmandu Valley, Nepal. *Journal of Hydrology: Regional Studies, 26*, 16.

LaMoreaux, P. E., Soliman, M. M., Memon, B. A., LaMoreaux, J. W., & Assaad, F. A. (2009). *Environmental Hydrogeology.* Boca Raton: CRC Press, Taylor & Francis Group.

Landon, J. (1991). *Booker tropical soil manual: A handbook for soil survey and agricultural land evaluation in the tropics and subtropics.* New York: John Wiley & Sons. Inc. .

Linsley, R., Kohler, M., & Paulhus, J. (1982). *Hydrology for engineers.* New York: McGraw-Hill.

Manandhar, S., Pandey, V. P., & Kazama, F. (2012, September). Hydro-climatic trends and hte people's perceptions: case of Kali Gandaki River Basin, Nepal. *Climate Research, Vol. 54*, 167-179. doi:doi: 10.3354/cr01108

Najim, M. M., Babel, M. S., & Loof, R. (2006). AGNPS Model Assessment for a Mixed Forested Watershed in Thailand. *Science Asia*, 53-61.

Parajuli, B. (2016). *Development of Flood Forecasting Model in Narayani River Basin, Nepal.* Technical Report, Department of Hydrology and Meteorology (DHM), Nepal, Kathmandu.

Penman, H. (1948). Natural evaporation from open water, bare soil and grass. *Proceedings of the Royal Society of London*, 24.

Poesen, J. (1984). Surface sealing as influenced by slope angle and position of simulated stones in the top layer of loose sediments. *Earth Surface Processes and Landforms*, 10.

Poulenard, J., Podwojewski, P., Janeau, J., & Collinet, J. (2001). Runoff and soil erosion under rainfall simulation of Andisols and from the Ecuadorian Paramo: effect of tillage and burning. *catena*, 23.

Rawls, W. J., Ahuja, L. R., Brakensiek, D. L., & Shirmohammadi, A. (1993). *Infiltration and soil water movement.* New York: McGraw Hill.

Richards, L. A. (1931). Capillary conduction through porous medium. *Physics 1*, 6.

Romkens, M. J., Luk, S. J., Poesen, J. W., & Mermut, A. R. (1995). Rain infiltration into loess soils from different geographic regions. *Elsevier*, 12.

Russo, D., & Bresler, E. (1982). Soil hydraulic properties as stochastic processes: Errors of estimated in a heterogeneous field. *Soil Science and America Journal/ Vol 46, Issue 1*.

Scharffenberg, W., Ely, P., Daly, S., Fleming, M., & Pak, J. (2010). Hydrological modelling system (HEC-HMS): Physically-based simulation components. *2nd Joint Federal Interagency Conference*, (p. 8). Las Vegas.

Simas, M. (1996). *Lag time characteristics in small watershed in the United States.* Arizona: University of Arizona.

Skaggs, R. W., & Khaleel, R. (1982). *Hydrology of small watersheds.* Michigan: St. Joseph.

Subramanya, K. (2008). *Engineering Hydrology.* India: McGraw Hill.

Turner, E. (2006). *Comparison of infiltration equations and their field validation with rainfall simulation.* USA: University of Maryland.

Xue, J., & Gavin, K. (2008). Effect of rainfall intensity on infiltration into partly saturated slopes. *Geotechnical and Geological Engineering*, 11.

Yimer, F., Messing, I., Ledin, S., & Abdelkadir, A. (2008). Effects of different landuse types on infiltration capacity in a catchment in the highlands of Ethiopia. *Soiil Use and Management*.

Zimmermann, B., & Elsenbeer, H. (2008). The near-surface hydrological consequences of disturbance and recovery: A simulation study. *Journal of Hydrology*.